

21-Telluraporphyrins. 3. Synthesis, Structure, and Spectral Properties of a 21,21-Dihalo-21-telluraporphyrin

Masako Abe, Michael R. Detty,* Oksana O. Gerlits, and Dinesh K. Sukumaran

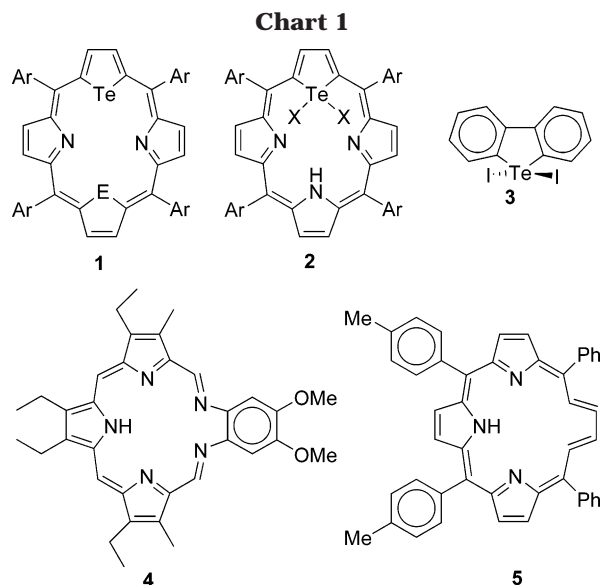
Department of Chemistry, University at Buffalo, The State University of New York,
Buffalo, New York 14260-3000

Received May 18, 2004

5,10-Diphenyl-15,20-di(4-methoxyphenyl)-21-telluraporphyrin (**7**) was prepared in 18% yield by the *p*-toluenesulfonic acid-catalyzed condensation of 2,5-bis(1-phenyl-1-hydroxymethyl)tellurophene (**6**), pyrrole, and 4-methoxybenzaldehyde in carefully deoxygenated CHCl₃ followed by oxidation with *p*-chloranil. While ¹H and ¹³C NMR spectra of **7** were consistent with a symmetrical molecule in solution, the X-ray crystal structure of **7** shows the pyrrole N-H on a pyrrole ring *cis* to the tellurophene and a planar porphyrin core. Air oxidation of a CH₂Cl₂ solution of **7** under fluorescent lighting gave telluroxide **14**. The reaction of a CH₂Cl₂ solution of **14** with 1 N HCl as a two-phase system gave 21,21-dichloro-21-telluraporphyrin **15**. The X-ray structure of **15** indicated a distorted trigonal bipyramidal geometry around the Te atom with two chloride ligands occupying the axial positions. The Te atom and the N atom of the *trans* pyrrole were tipped out of plane in opposite directions to give a nonplanar porphyrin core. The Q-bands of the absorption spectra of **15** and “vacataporphyrin” **5** were similar, suggesting a similar aromatic structure in the two molecules.

21-Core-modified porphyrins are formed by replacing a pyrrole NH group with a chalcogen atom: O, S, Se, or Te.^{1–3} Of these molecules, the 21-telluraporphyrins **1** (Chart 1) have several interesting structural features. The size of the Te atom essentially fills the core and prevents metals from binding within the core of the 21-telluraporphyrin. Although the Te⋯N distance of 3.13 Å observed between the Te atom and the N atom of the *trans*-pyrrole in one 21-telluraporphyrin is quite short,² the porphyrin macrocycle remains essentially planar, which suggests that the electronic structure of the porphyrin core is maintained. In the Te(II) oxidation state, the Te 5p orbital overlaps with the carbon π-framework to maintain the full porphyrin aromaticity.

Oxidative addition of halogen to a 21-telluraporphyrin would generate the corresponding 21,21-dihalo-21-telluraporphyrin **2**. In the Te(IV) oxidation state, the two axial halogen ligands on the Te atom would prevent the Te 5p orbital from overlapping with the carbon π-framework. While structures such as **2** have yet to be reported in the 21-telluraporphyrins, the X-ray crystal structure of dibenzotellurophene diiodide **3** (Chart 1) shows a nearly linear I–Te–I array parallel to the carbon π-framework of the dibenzotellurophene.⁴ If a similar oxidative addition was to occur in the 21-telluraporphyrins, the resulting porphyrin-like molecules might be expected to have unusual electronic properties by effectively removing the Te atom from the porphyrin aromaticity. The core-expanded porphyrins or “texa-



phyrins” such as **4**⁵ and “vacataporphyrin” **5**⁶ (Chart 1) are porphyrin-like molecules that have removed the N atom from one pyrrole from the porphyrin chromophore. The spectral properties of **4** and **5** differ markedly from their porphyrin counterparts.

The only Te(IV) derivatives among the 21-telluraporphyrins to be described and characterized are the corresponding telluroxides of the 21-telluraporphyrins.^{2,3,6,7} Attempts to prepare 21,21-dihalo-21-tellu-

* Corresponding author. E-mail: mdetty@buffalo.edu.

(1) Ulman, A.; Manassen, J.; Frolow, F.; Rabinovich, D. *Tetrahedron Lett.* **1978**, 1885.

(2) Latos-Grazyński, L.; Pacholska, E.; Chmielewski, P. J.; Olmstead, M. M.; Balch, A. L. *Angew. Chem., Int. Ed. Engl.* **1995**, *34*, 2252.

(3) Abe, M.; Hilmey, D. G.; Stilts, C. E.; Sukumaran, D. K.; Detty, M. R. *Organometallics* **2002**, *21*, 2986.

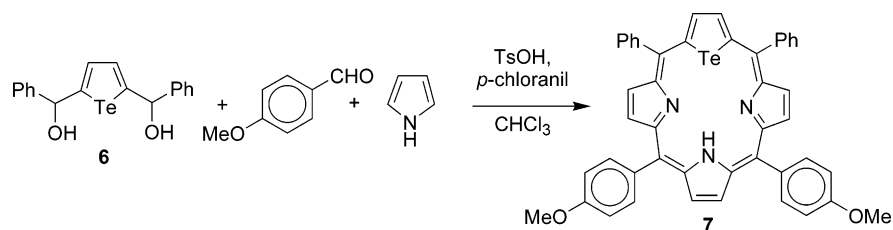
(4) McCullough, J. D. *Inorg. Chem.* **1975**, *14*, 1142.

(5) (a) Sessler, J. L.; Hemmi, G.; Mody, T. D.; Murai, T.; Burrell, A.; Young, S. W. *Acc. Chem. Res.* **1994**, *27*, 43–50. (b) Hannah, S.; Lynch, V. M.; Gerasimchuk, N.; Magda, D.; Sessler, J. L. *Org. Lett.* **2001**, *3*, 3911.

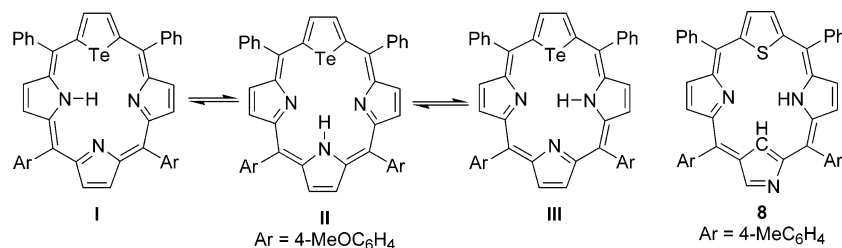
(6) Pacholska, E.; Latos-Grazyński, L.; Ciunik, Z. *Chem. Eur. J.* **2002**, *8*, 5403.

(7) Abe, M.; You, Y.; Detty, M. R. *Organometallics* **2002**, *21*, 4546.

Scheme 1



Scheme 2



raporphyrins by direct oxidative addition of halogen have not given the expected compounds, but only monohalogenated derivatives.⁷ Herein, we describe a novel approach to the synthesis of a 21,21-dihalo-21-telluraporphyrin: oxidation of 21-telluraporphyrin to its corresponding telluroxide and ligand exchange with chloride in an HCl solution to give a 21,21-dichloro-21-telluraporphyrin.

Results and Discussion

Preparation of 21-Telluraporphyrin 7. The condensation of 2,5-bis(1-phenyl-1-hydroxymethyl)tellurophene (**6**), pyrrole, and 4-methoxybenzaldehyde with *p*-toluenesulfonic acid in carefully deoxygenated CHCl_3 followed by oxidation with *p*-chloranil gave 21-telluraporphyrin **7** in 18% isolated yield as shown in Scheme 1.⁶ The spectral properties of **7** were consistent with those of other 21-telluraporphyrins.^{1–3}

As shown in Scheme 2, three different tautomeric forms are possible for 21-telluraporphyrin **7** with each one placing the pyrrole NH on a different pyrrole ring. Tautomer **II** is symmetric with an axis of symmetry and a plane of symmetry along the $\text{Te}\cdots\text{H}-\text{N}$ array. Tautomers **I** and **III** are spectroscopically identical, but lack the symmetry elements contained in **II**. At 296 ± 1 K, the ^1H and ^{13}C NMR spectra of **7** are those of a symmetrical molecule. At 218 ± 1 K, the ^1H NMR spectrum of a CDCl_3 solution of **7** displayed no changes consistent with the slowing of an exchange process. These data suggest either that contributions from tautomers **I** and **III** are minor to the composition of **7** between 218 and 296 K or that interconversion of the three tautomers is rapid on the NMR time scale.

Crystals of **7** were characterized by X-ray crystallography as shown in Figure 1. One phenyl ring was rotationally disordered into two positions with the population of each refined to 54/46%. The crystal structure revealed one surprising structural feature not observed in the structures of other 21-telluraporphyrins.² The X-ray structure of **7** clearly is that of tautomer **I/III** of Scheme 2 with the pyrrole N-H on a pyrrole ring *cis* to the tellurophene. The H atom on N3 was located from the difference electron density map, and its posi-

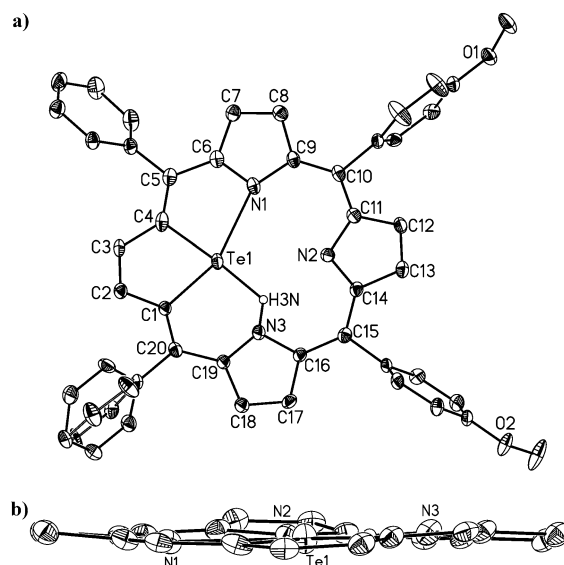


Figure 1. Molecular structure of compound **7** (ellipsoids are drawn with 50% probability) viewed (a) from the top and (b) from the side with aryl groups omitted for clarity.

tion was refined. The Te atom interacts with the H atom on N3 through hydrogen bonding with a $\text{Te1}\cdots\text{HN3}$ distance of 1.827 Å. The Te atom also interacts strongly with N1 on the second *cis*-pyrrole ring with a $\text{Te1}\cdots\text{N1}$ distance of 2.558 Å. The $\text{Te}\cdots\text{N2}$ distance of 3.173 Å is nearly identical to the $\text{Te}\cdots\text{N}$ distance of 3.13 Å observed in a related 21-telluraporphyrin.² As observed in other 21-telluraporphyrins, the $\text{N1}\cdots\text{N3}$ distance is elongated (4.644 Å) relative to a normal porphyrin to accommodate the size of the Te atom.² As shown in Figure 1b, the overall conformation of the macrocycle is only slightly distorted from planarity. A closely related structure is observed for thia N-confused porphyrin **8** (Scheme 2),⁸ in which the HN is equally distributed on both pyrroles *cis* to the thiophene.

21,21-Dichloro-21-Telluraporphyrin 15. Oxidation of 21-telluraporphyrins gives stable Te(IV) (telluroxide) states.^{2,7} Many diorgano telluroxides readily undergo

(8) Pushpin, S. K.; Srinivasan, A.; Anand, V. R. G.; Chandrashekar, T. K.; Subramanian, A.; Roy, R.; Sugiyra, K.; Sakata, Y. *J. Org. Chem.* **2001**, *66*, 153.

Scheme 3

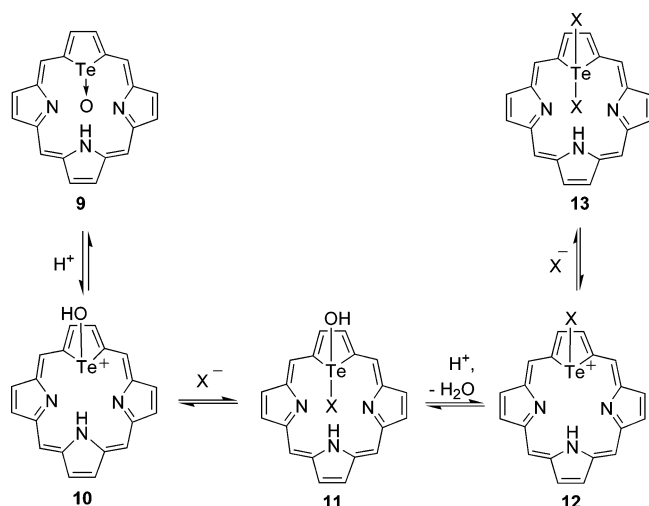
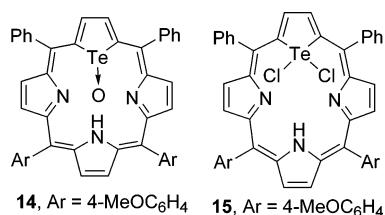


Chart 2



addition of water to give the corresponding diorgano dihydroxy Te(IV) telluranes. These molecules undergo ligand exchange with halide salts to give halotellurium intermediates and/or dihalo Te(IV) compounds.^{7,9} We viewed the exchange of halide ligands for hydroxy ligands in the telluroxide/dihydroxy tellurane oxidation state as a viable entry to the 21,21-dihalo-21-telluraporphyrins as shown in Scheme 3.

The oxides of 21-telluraporphyrins such as **9** have an unusual structure.² When viewed from the side, the tellurophene ring and the *trans* pyrrole ring are tipped out of plane in opposite directions. The telluroxide O projects back through the porphyrin plane and is protonated by or forms a strong hydrogen bond to the pyrrole NH *trans* to the tellurophene ring. Under mildly acidic conditions, protonation of telluroxide **9** should give protonated telluroxide **10** with a protonated pyrrole N. Addition of a halide ion to the hydroxytelluronium intermediate **10** would give tellurane **11** as shown in Scheme 3.^{9a} Protonation of **11** and loss of water would then give halotelluronium intermediate **12**, which would then add a second halide to give a 21,21-dihalo-21-telluraporphyrin, **13**.

The oxidation of 21-telluraporphyrins to 21-oxo-21-telluraporphyrins has been accomplished via air oxidation,² 3-chloroperoxybenzoic acid,² and hydrogen peroxide.³ The air oxidation of **7** to the corresponding telluroxide **14** (Chart 2) was not without ambiguity. The air oxidation of **7** as a stirred solution, but in an open foil-covered flask to exclude light, was very slow, with less than 10% reaction after 48 h. However, stirring a 3×10^{-3} M solution of **7** in THF exposed to overhead fluorescent room lights for several hours gave complete

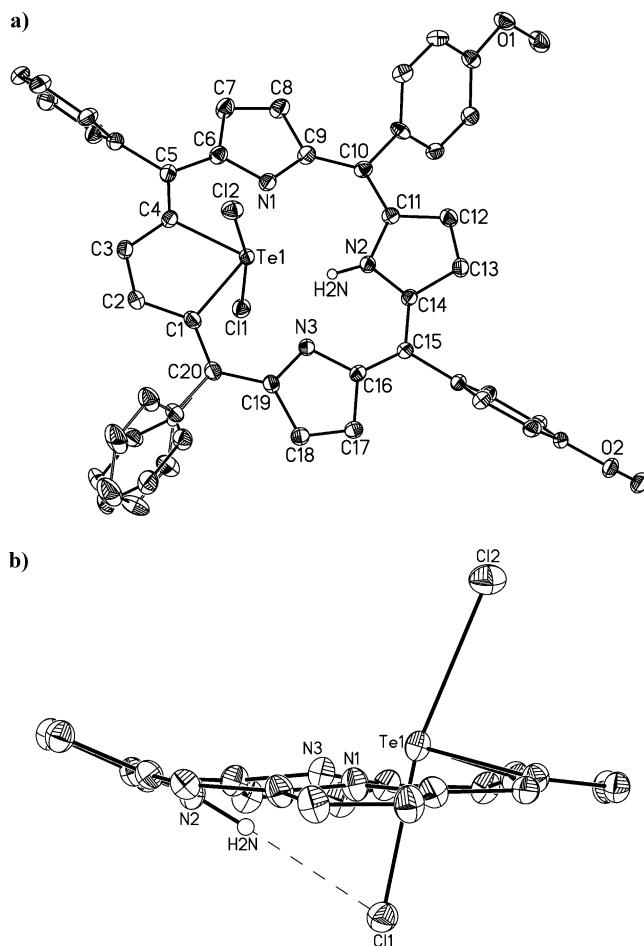


Figure 2. Molecular structure of compound **15** (ellipsoids are drawn with 50% probability) viewed (a) from the top and (b) from the side with aryl groups omitted for clarity.

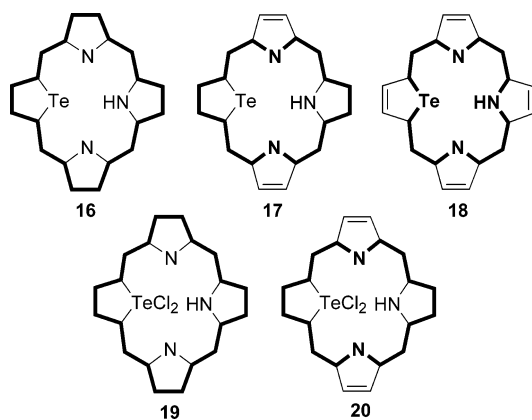
oxidation of **7** to **14**, which was isolated in 94% yield. The rapid reaction of **7** with singlet oxygen generated by self-sensitization hinders accurate determination of quantum yields for singlet oxygen generation [$\phi(^1O_2)$] with **7**. However, other core-modified porphyrins containing S and Se atoms have been efficient generators of singlet oxygen [$\phi(^1O_2)$ of 0.50 to 0.87] upon exposure to light,¹⁰ and one would expect a 21-telluraporphyrin derivative such as **7** to also generate singlet oxygen efficiently, as well. Self-sensitized generation of singlet oxygen by **7** upon exposure to light is most likely responsible for the oxidation of **7** to **14**.

Stirring a two-phase system of **14** in CH_2Cl_2 and 1 N HCl for several seconds gave complete conversion of **14** to 21,21-dichloro-21-telluraporphyrin **15**. Crystals of **15** were isolated by concentration of the CH_2Cl_2 layer and recrystallization of the crude product from $CHCl_3/EtOH$. The black, parallelepiped crystals of **15** were characterized by X-ray crystallography, as shown in Figure 2. The Te atom of **15** is in the Te(IV) oxidation state with two Cl atoms attached in the axial positions to Te in the center of a trigonal bipyramid. The Cl1–Te1–Cl2 bond angle of 168.65° reflects the stereochemically active lone

(9) (a) Detty, M. R.; Zhou, F.; Friedman, A. E. *J. Am. Chem. Soc.* **1996**, *118*, 313. (b) Higgs, D. E.; Nelen, M. I.; Detty, M. R. *Org. Lett.* **2001**, *3*, 349.

(10) (a) Hilmey, D. G.; Abe, M.; Nelen, M. I.; Stilts, C. E.; Baker, G. A.; Baker, S. N.; Bright, F. V.; Davies, S. R.; Gollnick, S. O.; Oseroff, A. R.; Gibson, S. L.; Hilf, R.; Detty, M. R. *J. Med. Chem.* **2002**, *45*, 449. (b) You, Y.; Gibson, S. L.; Hilf, R.; Davies, S. R.; Oseroff, A. R.; Roy, I.; Ohulchanskyy, T. Y.; Bergey, E. J.; Detty, M. R. *J. Med. Chem.* **2003**, *46*, 3734.

Chart 3



pair of electrons on Te1 in the equatorial plane of the trigonal bipyramid. The Te–Cl bonds are not equal in length, with the Te1–Cl2 bond (2.58 Å) elongated relative to the “normal” (2.447–2.538 Å)¹¹ Te1–Cl1 bond length of 2.49 Å. The tellurophene ring is distorted from planarity with Te1 displaced from the plane of the four carbons by 0.281 Å toward Cl2 (Figure 2b). The hydrogen atom at N2 was located from the difference electron density map and was not refined further. The N2 atom has a flattened trigonal pyramidal configuration (the sum of bond angles is 364.3°). The Cl1 atom forms a strong hydrogen bond to HN2 with a Cl1⋯HN2 distance of 2.349 Å. The overall conformation of the 21-telluraporphyrin is nonplanar, which is in contrast to the planarity observed in **7** (Figure 1b).

The structure of **15** is very similar to the reported structure of a 21-telluraporphyrin telluroxide.² Both Te1 and N2 are tipped out of plane in opposite directions, as was reported for the telluroxide.² The Te1–Cl1 bond projects back through the core through the plane of the core-modified porphyrin, and the hydrogen atom HN2 on the pyrrole *trans* to the tellurophene is hydrogen bonded to Cl1.

The Te1⋯N2 distance of 3.293 Å in **15** is somewhat longer than the Te1⋯N2 distance (3.173 Å) in **7** and is most likely due to the fact that the Te1 and N2 atoms in **15** are tipped out of plane in opposite directions. However, the N1⋯N3 distance of 4.625 Å in **15** is nearly identical to the N1⋯N3 distance (4.644 Å) in **7**. In both examples, the elongated N1⋯N3 distance accommodates the large Te atom.

The Electronic Similarity of 15 and “Vacataporphyrin” 5. The aromaticity of the porphyrin macrocycle has contributions from several different annulene-type structures.^{12,13} The Te atom of **7** is part of the 21-telluraporphyrin π -framework, and the annulene components **16**–**18** (Chart 3) contribute to the overall electronic configuration of **7**. In 21,21-dichloro-21-telluraporphyrin **15**, no telluraannulene contributions from a structure comparable to **18** are possible, and porphyrin aromatic delocalization is limited to contributions from

Table 1. Absorption Bands of “Vacataporphyrin” 5, 21-Telluraporphyrin 7, and 21,21-Dichloro-21-telluraporphyrin 15

	5, nm (ϵ , M ⁻¹ cm ⁻¹) ^a	7, nm (ϵ , M ⁻¹ cm ⁻¹) ^b	15, nm (ϵ , M ⁻¹ cm ⁻¹) ^b
band 1	742 (1260)	687 (6700)	742 (5100)
band 2	672 (790)	624 (5600)	669 (3100)
band 3	611 (630)	578 (sh, 7200)	583 (8000)
band 4	522 (6300)	536 (19 300)	550 (18 000)
band 5	489 (2500)		
Soret band	433 (50 100)	443 (219 000)	468 (125 000)

^a Data from ref 6. ^b In dichloromethane.

annulene **19** and diazaannulene **20** (Chart 3). Structurally, the π -framework of **15** should be very similar to that of “vacataporphyrin” **5** (Chart 1).⁶

The π -framework similarity is demonstrated in a comparison of the electronic absorption spectra of **5** and **15**. The absorption spectra of “vacataporphyrin” **5**, 21-telluraporphyrin **7**, and 21,21-dichloro-21-telluraporphyrin **15** are summarized in Table 1. The maxima for Q-bands 1–4 are nearly identical for **15** and “vacataporphyrin” **5**, which suggests a similar electronic structure in the two molecules. The absorption spectrum of **7** is quite different than that of either **5** or **15**. The band 1 maximum of **7** is at 55 nm shorter wavelength than the band 1 maximum of either **5** or **15**.

¹²⁵Te NMR Spectra. The ¹²⁵Te NMR spectra of **7**, **14**, and **15** were acquired at 126.289 MHz and 55 °C. The Te(II) derivative **7** gave a ¹²⁵Te NMR signal at δ 823.6. Oxidation of **7** to the Te(IV) oxide **14** gave a downfield shift in the ¹²⁵Te NMR signal to δ 1046.3. Surprisingly, the ¹²⁵Te NMR signal of 21,21-dichloro-21-telluraporphyrin **15** is observed at δ 793.9, which is actually at higher field than the Te(II) derivative **7**. As a point of reference, the ¹²⁵Te NMR signal for tellurophene is at δ 793.¹⁴

Typically, the ¹²⁵Te NMR chemical shifts of dihalo-tellurium(IV) derivatives are at lower field than the corresponding tellurium(II) derivatives, as observed with **7** and **14**.^{15,16} However, there are exceptions to this generalization, and these exceptions are typically found in systems where charge delocalization/localization changes between the Te(II) and Te(IV) derivatives of a particular π -framework. Values of the ¹²⁵Te NMR chemical shift are particularly sensitive to the buildup of positive charge in the molecule. As an example, telluropyran **21** (Chart 4) is a neutral Te(II) compound with a ¹²⁵Te NMR chemical shift of δ 257 (vs δ 0.0 for the ¹²⁵Te NMR chemical shift of Me₂Te).^{16a} Hydride abstraction gives the telluropyrylium salt **22** (Chart 5) with a ¹²⁵Te NMR chemical shift of δ 1304! The telluropyranone **23** (Chart 5) has one resonance form that delocalizes positive charge to the Te atom, as shown in Chart 5 with the resulting ¹²⁵Te NMR chemical shift of δ 445. However, the dihalo Te(IV) derivatives **24** and **25** (Chart 5) do not have comparable resonance forms to place charge on Te, and the corresponding ¹²⁵Te NMR chemical shifts of the Te(IV) derivatives are actually at

(11) (a) Detty, M. R.; Murray, B. J.; Smith, D. L.; Zumbulyadis, N. *J. Am. Chem. Soc.* **1983**, *105*, 875. (b) Dupont, L.; Diderberg, O.; Lamotte, J.; Piette, J. L. *Acta Crystallogr.* **1979**, *B35*, 84. (c) Singh, H. B.; Sudha, N.; Butcher, R. T. *Inorg. Chem.* **1992**, *31*, 1431.

(12) (a) Michl, J. *J. Am. Chem. Soc.* **1978**, *100*, 6801. (b) Waluk, J.; Michl, J. *J. Org. Chem.* **1991**, *56*, 2729.

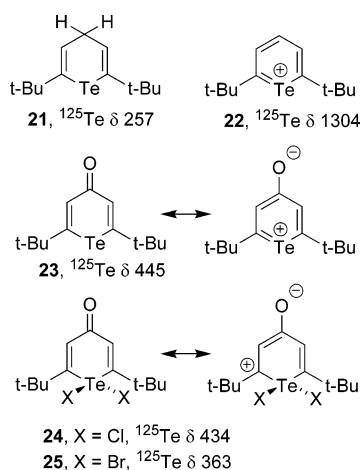
(13) (a) Cyrański, M. K.; Krygowski, T. M.; Wisiorowski, M.; van Eikema Hommes, N. J. R.; von Rague Schleyer, P. *Angew. Chem. Int. Ed.* **1998**, *37*, 177. (b) Vogel, E. *J. Heterocycl. Chem.* **1996**, *33*, 1461.

(14) Martin, M. L.; Trierweiler, M.; Galasso, V.; Fringuelli, F.; Taticchi, A. *J. Magn. Reson.* **1982**, *47*, 504.

(15) Detty, M. R.; O'Regan, M. B. Tellurium-Containing Heterocycles. In *The Chemistry of Heterocyclic Compounds*; Taylor, E. C., Ed.; Wiley-Interscience: New York, 1994; Vol. 53.

(16) (a) Detty, M. R.; Lenhart, W. C.; Gassman, P. G.; Callstrom, M. R. *Organometallics* **1989**, *8*, 861. (b) Detty, M. R.; Lenhart, W. C.; Gassman, P. G.; Callstrom, M. R. *Organometallics* **1989**, *8*, 866.

Chart 4



higher field at δ 434 and 363, respectively, relative to the Te(II) derivative **23**.

One might reasonably query whether the trends observed in the ^{125}Te chemical shifts of **7**, **14**, and **15** were unusual. The Te atom in the tellurophene ring of **7** is part of an aromatic system, and the ^{125}Te shift might be shifted downfield due to the ring current. The ^{125}Te chemical shifts observed for **7** and tellurophene (δ 793)¹⁴ are actually quite similar. Oxidation of **7** to the telluroxide **14** gives a 223 ppm downfield shift in the ^{125}Te NMR signal, which is consistent with a more electron-deficient Te(IV) center bearing an electron-withdrawing O atom and a formal charge separation as $\text{R}_2\text{Te}^+-\text{O}^-$. The telluroxide is no longer part of an aromatic tellurophene ring (loss of the conjugation to the 5p orbital of Te), so the downfield contribution from this aromaticity is lost and the downfield shift reflects the buildup of positive charge.

The 21,21-dichloro Te(IV) derivative **15** neutralizes the formal positive charge on the Te atom of **14** via the addition of the second chloride ligand, and the resulting ^{125}Te NMR chemical shift of **15** is shifted upfield by 252 ppm. Part of the upfield shift observed in **15** is perhaps due to annulene contributions from **19** and **20** (Chart 4), where the Te(IV) would be in the shielding core of the diamagnetic ring current of the macrocycle. In the ^1H NMR spectrum of "vacataporphyrin" **5**, the two olefinic protons in the annulene core were observed at δ -2.5 and the N-H of the pyrrole was observed at δ 0.01, which is consistent with a diamagnetic ring current in **5**.⁶ The chemical shift of the N-H proton of **15** was shifted downfield at δ 1.66 in the ^1H NMR spectrum of **15**, which is consistent with the hydrogen bond between the NH and the one chloride ligand. The potential for a diamagnetic ring current in **15** having been acknowledged, the upfield ^{125}Te NMR chemical shift observed with **15** also has significant contributions from the loss of tellurophene aromaticity upon oxidative addition.

Summary

Although 21,21-dichloro-21-telluraporphyrin **15** is not readily prepared by the oxidative addition of chlorine to 21-telluraporphyrin **7**, the reaction of the corresponding telluroxide **14** with HCl gives **15** in excellent yield. The telluroxide **14** and 21,21-dichloro-21-telluraporphyrin

15 both have tellurium in the Te(IV) oxidation state, and the reaction of HCl with **14** to produce **15** represents on net a ligand exchange reaction. The structure of **15** was confirmed by X-ray crystallographic analysis. The absorption spectrum of "vacataporphyrin" **5**,⁶ which suggests a similar electronic structure for the two molecules. The ^1H and ^{125}Te NMR spectra of **15** are consistent with contributions from (a) a diamagnetic ring current from annulene contributions like **19** and **20** to the overall electronic structure of **15**, (b) loss of tellurophene aromaticity in **15**, and (c) hydrogen bonding of the pyrrole NH to a chloride ligand of Te(IV) giving a downfield ^1H NMR chemical shift for the pyrrole NH.

The crystal structure of **7** was of a tautomer with the pyrrole NH *cis* to the tellurophene ring in the 21-telluraporphyrin. This tautomer has not been previously characterized in the 21-telluraporphyrins.

Experimental Section

General Methods. Solvents and reagents were used as received from Sigma-Aldrich Chemical Co. (St. Louis, MO) unless otherwise noted. Concentration *in vacuo* was performed on a Büchi rotary evaporator. NMR spectra were recorded at 293.0 K on a Varian Gemini-300, Inova-400, or Inova-500 NMR spectrometer with residual solvent signal as internal standard: CDCl_3 (δ 7.26 for proton, δ 77.0 for carbon). UV-visible-near-IR spectra were recorded on a Perkin-Elmer Lambda 12 spectrophotometer. Elemental analyses were conducted by Atlantic Microlabs, Inc. High-resolution Q-TOF mass spectrometry was conducted by the Campus Chemical Instrumentation Center of The Ohio State University. Compound **6** was prepared as described in ref 2.

Preparation of 5,10-Diphenyl-15,20-di-4-methoxyphenyl-21-telluraporphyrin (7). A solution of 2,5-bis(1-phenyl-1-hydroxymethyl)tellurophene (**6**,² 0.783 g, 2.00 mmol), pyrrole (0.72 mL, 11 mmol), and 4-methoxybenzaldehyde (0.84 mL, 5.5 mmol) in 450 mL of CHCl_3 was degassed under a stream of argon bubbles. The reaction vessel was covered with aluminum foil. *p*-Toluenesulfonic acid (0.39 g, 2.0 mmol) was added, and the resulting solution was stirred at ambient temperature for 1 h. *p*-Chloranil (2.26 g, 9.2 mmol) was added, and the resulting mixture was heated at reflux for 1 h. The reaction mixture was cooled to ambient temperature and concentrated *in vacuo*. The residue was purified via chromatography on basic alumina eluted with CH_2Cl_2 in a foil-wrapped column. The first bands were rechromatographed on silica gel eluted with CH_2Cl_2 , and the first, red-brown band was collected. The dark purple product was washed with 1:1 acetone/methanol to give 283 mg (18%) of **7**, mp >300 °C: ^1H NMR (400 MHz, CDCl_3) δ 10.41 (s, 2 H), 8.64 (s, 2 H), 8.585 (br s, 4 H), 8.24 (d, 4 H, $J = 7.6$ Hz), 8.16 (d, 4 H, $J = 7.6$ Hz), 7.83 (dd, 4 H, $J = 7.2, 7.6$ Hz), 7.74 (t, 2 H, $J = 7.2$ Hz), 7.31 (d, 4 H, $J = 7.6$ Hz), 4.105 (s, 6 H), -1.41 (br s, 1 H); ^{13}C NMR (CDCl_3) δ 160.94, 159.87, 153.73, 150.78, 141.17, 140.55, 140.31, 137.39, 136.24, 135.61, 134.04, 130.77, 127.93, 127.53, 127.32, 125.94, 112.30, 55.62 (overlap of two signals); ^{125}Te NMR (126 MHz, CDCl_3) δ 823.6; λ_{max} (ϵ , $\text{M}^{-1} \text{cm}^{-1}$) 443 (2.19×10^5), 536 (1.93×10^4), 578 (sh, 7.2×10^3), 624 (5.6×10^3), 687 (6.7×10^3). Anal. Calcd for $\text{C}_{46}\text{H}_{33}\text{N}_3\text{O}_2\text{Te}$: C, 70.17; H, 4.22; N, 5.34. Found: C, 69.93; H, 4.13; N, 5.35.

Oxidation of 7. A solution of **7** (50.0 mg, 63.5 μmol) in 200 mL of freshly distilled THF was stirred open to the air and exposed to overhead fluorescent light fixtures for several hours until oxidation of starting material was complete by TLC. Comparable results were obtained in CH_2Cl_2 . After concentration of solvent, the green solid was collected by filtration, washed with acetone, and dried to give 48 mg (94%) of **14** as

a green solid, mp > 300 °C: ^1H NMR (400 MHz, CDCl_3) δ 10.42 (s, 2 H), 8.48 (d, 2 H, $J = 4.4$ Hz), 8.41 (d, 2 H, $J = 4.4$ Hz), 8.31 (s, 2 H), 8.24 (br d, 4 H, $J = 6.8$ Hz), 8.09 (br d, 2 H, $J = 7.6$ Hz), 8.04 (br d, 2 H, $J = 7.6$ Hz), 7.83 (t, 4 H, $J = 7.6$ Hz), 7.74 (t, 2 H, $J = 7.6$ Hz), 7.24 (d, 4 H, $J = 8.8$ Hz), 4.08 (s, 6 H), -1.48 (br s, 1 H); ^{13}C NMR (75 MHz, CDCl_3) δ 159.56, 156.98, 155.16, 146.35, 141.59, 139.07, 137.79, 137.56, 136.98 (br), 136.16, 135.40, 133.26, 132.89, 128.46, 126.08 (br), 111.73, 55.56 (overlap of some signals); ^{125}Te NMR (126 MHz, CDCl_3) δ 1046.3; λ_{max} (ϵ , $\text{M}^{-1} \text{cm}^{-1}$) 465 (8.3×10^4), 486 (5.66×10^4), 567 (5.5×10^3), 658 (1.57×10^4), 693 (sh, 4.5×10^3). Anal. Calcd for $\text{C}_{46}\text{H}_{33}\text{N}_3\text{O}_2\text{Te} \cdot 3\text{H}_2\text{O}$: C, 64.44; H, 4.58; N, 4.90. Found: C, 64.55; H, 4.31; N, 4.61.

Preparation of 21,21-Dichloro-5,10-diphenyl-15,20-di-4-methoxyphenyl-21-telluraporphyrin (15). A two-phase mixture of **14** (27.0 mg, $63.5 \mu\text{mol}$) in 50 mL of CH_2Cl_2 and 5 mL of 1.0 N HCl was stirred at ambient temperature for 30 s until the initial green color of the mixture turned to red. The CH_2Cl_2 layer was washed with brine and dried over MgSO_4 . The reaction mixture was concentrated to give a purple solid, which was collected by filtration to give 22 mg (76%) of **15**. The crude crystals were recrystallized from 1:1 chloroform/ethanol to give a deep purple solid, mp > 300 K: ^1H NMR (400 MHz, CDCl_3) δ 10.24 (s, 2 H), 8.33 (d, 2 H, $J = 4.8$ Hz), 8.25 (d, 2 H, $J = 4.8$ Hz), 8.15 (d, 4 H, $J = 6.9$ Hz), 8.09 (d, 4 H, $J = 8.4$ Hz), 7.96 (d, 2 H, $J = 1.5$ Hz), 7.76 (m, 6 H), 7.32 (d, 4 H, $J = 8.4$ Hz), 4.09 (s, 6 H), 1.66 (br s, 1 H); ^{13}C NMR (75 MHz, CDCl_3) δ 162.14, 160.76, 152.26, 150.56, 142.35, 141.06, 139.37, 138.03, 137.42, 136.59, 134.57, 133.61, 132.68, 129.75, 128.45, 126.30, 112.90, 55.65 (overlap of two signals); ^{125}Te (126 MHz, CDCl_3) δ 793.9; λ_{max} (ϵ , $\text{M}^{-1} \text{cm}^{-1}$) 468 (1.25×10^5), 550 (1.80×10^4), 583 (8.0×10^3), 669 (3.10×10^3), 742 (5.1×10^3). Anal. Calcd for $\text{C}_{46}\text{H}_{33}\text{N}_3\text{O}_2\text{Te} \cdot 0.5\text{CHCl}_3 \cdot 0.25\text{EtOH}$: C, 60.72; H, 3.80; N, 4.52. Found: C, 60.92; H, 3.84; N, 4.46. (Note: the solvents of crystallization were observed in the crystal structure of **15**.)

Acquisition of ^{125}Te NMR Spectra. The NMR samples were prepared in CDCl_3 in 5 mm NMR tubes. The ^{125}Te NMR spectra were recorded on a Varian Inova-400 NMR spectrometer at 126.289 MHz and 55 °C. The spectral width for acquisition was set to 320 kHz with an acquisition time of 0.82 s. The data were collected for 16K transients, with a pulse width of 9 μs and a relaxation delay of 3–4 s. The FIDs were transformed with an exponential line broadening function of 10–15 Hz.

X-ray Diffraction Data. X-ray diffraction data on **7** and **15** were collected at 90 ± 1 K using a Bruker SMART 1000 CCD diffractometer installed at a rotating anode source (Mo $\text{K}\alpha$ radiation, $\lambda = 0.71073$ D) and equipped with an Oxford Cryosystems nitrogen gas-flow apparatus. The data were collected by the rotation method with 0.3d frame-width (ω scan) and 60 s exposure time per frame for **7** and 10 s exposure time per frame for **15**. Four sets of data (600 frames in each set) were collected, nominally covering half of reciprocal space. The data were integrated, scaled, sorted, and averaged using the SMART software package.¹⁷ The structure was solved by direct methods using SHELXTL NT version 5.10.¹⁸ The structure was refined by full-matrix least squares against F^2 .

For 7. Non-hydrogen atoms were refined anisotropically. One phenyl ring is rotationally disordered into two positions with populations refined to 54/46%. Positions of hydrogen atoms were found by difference electron density Fourier synthesis. The CH_3 hydrogens were treated as part of idealized CH_3 groups with $U_{\text{iso}} = 1.5U_{\text{eq}}$, while the remainder of the hydrogen atoms were refined with the “riding” model with U_{iso}

Table 2. Crystallographic Data for 7 and 15

	7	15
formula	$\text{C}_{46}\text{H}_{33}\text{N}_3\text{O}_2\text{Te}$	$\text{C}_{46.90}\text{H}_{34.65}\text{Cl}_{3.20}\text{N}_3\text{O}_{2.25}\text{Te}$
M_r [g mol^{-1}]	787.35	917.27
cryst shape	plate	parallelepiped
cryst syst	monoclinic	monoclinic
space group	$C2/c$	$P2_1/c$
a [\AA]	35.658(1)	18.8613(8)
b [\AA]	12.4853(4)	10.7521(5)
c [\AA]	18.0090(6)	21.3737(9)
α [deg]	90	90
β [deg]	116.482(1)	93.159(1)
γ [deg]	90	90
V [\AA^3]	7176.4(4)	4328.0(3)
Z	8	4
ρ_{calc} [g cm^{-3}]	1.457	1.408
μ [mm^{-1}]	0.873	0.926
T [K]	90(1)	90(1)
λ [\AA]	0.71073	0.71073
max. 2θ [deg]	54	64
abs corr method	SADABS 2.05	SADABS 2.05
no. of reflns	27 934	85 957
measd		
no. of unique reflns (R_{int})	7738 (0.0643)	15 014 (0.0595)
no. of reflns $I > 4\sigma(I)$	5357	11 086
no. of params refined	510	553
R [$I > 2\sigma(I)$]	0.0361	0.0457
wR_2	0.0890	0.1303
GOF	0.999	1.089

$= 1.2U_{\text{eq}}$. Crystallographic data are compiled in Table 2. Atomic coordinates, anisotropic displacement parameters, and bond lengths and angles are given in Tables S1, S2, and S3, respectively, of the Supporting Information.

For 15. The majority of non-hydrogen atoms were refined anisotropically. One phenyl ring and one partially occupied CHCl_3 solvent molecule are disordered into two equally occupied positions. The disordered phenyl rings were constrained geometrically to be ideal hexagons with 1.390 \AA $\text{C}_{\text{Ar}}-\text{C}_{\text{Ar}}$ bonds. All atoms of the disordered solvent molecules (CHCl_3 , EtOH) were refined isotropically, while the bonds in chloroform and the $\text{C3S}-\text{O1S}$ bond in ethanol were constrained to their ideal values of 1.790 and 1.426 \AA , respectively.¹⁹ Positions of hydrogen atoms were found by difference electron density Fourier synthesis. The CH_3 hydrogens were treated as part of idealized CH_3 groups with $U_{\text{iso}} = 1.5U_{\text{eq}}$, while the remainder of the hydrogen atoms were refined with the “riding” model with $U_{\text{iso}} = 1.2U_{\text{eq}}$. Crystallographic data are compiled in Table 2. Atomic coordinates, anisotropic displacement parameters, and bond lengths and angles are given in Tables S4, S5, and S6, respectively, of the Supporting Information.

Acknowledgment. The authors thank the Office of Naval Research and the National Science Foundation for grants in support of this work.

Supporting Information Available: Table S1 (atomic coordinates and displacement parameters for **7**), Table S2 (anisotropic displacement parameters for **7**), Table S3 (bond lengths and angles for **7**), Table S4 (atomic coordinates and equivalent isotropic displacement parameters for **15**), Table S5 (anisotropic displacement parameters for **15**), and Table S6 (bond lengths and angles for **15**). This information is available free of charge via the Internet at <http://pubs.acs.org>.

OM049640R

(19) Allen, F. H.; Kennard, O.; Watson, D. G.; Brammer, L.; Orpen, A. J.; Taylor, R. *J. Chem. Soc., Perkin Trans. 2* **1987**, 1.

(17) SMART and SAINTPLUS, Area detector control and integration software, Ver. 6.01; Bruker Analytical X-ray Systems: Madison, WI, 1999.

(18) SHELXTL, An integrated system for solving, refining and displaying crystal structures from diffraction data, Ver. 5.10; Bruker Analytical X-ray Systems: Madison, WI, 1997.